MAUSAM, **76**, 3 (July 2025), 824-839

MAUSAM

DOI : https://doi.org/10.54302/mausam.v76i3.6265
Homepage: https://mausamjournal.imd.gov.in/index.php/MAUSAM

UDC No.502.3:614.4(511.1)

Analysis of CO_2 over Hubei of China in the first round of COVID-19 scenarios

XUEFU DAN[1,2#], XULONG WU[1,2@], JINYE ZHANG[1,2*], RUIBEI LIU[3], ZIYUE HU[1,2$] and CHANG XU[1,2&]

[1]*School of Science, Hubei University of Technology, Wuhan 430 068, China*

[2]*Hubei Collaborative Innovation Center for High-efficiency Utilization of Solar Energy,*

Hubei University of Technology, Wuhan 430 068, China

([#]470479985@qq.com; [@]longerwood0218@163.com; [$]liuruibei@hbou.edu.cn; [&]764451213@qq.com)

[3]*School of Software Engineering, Hubei Open University, Wuhan 430 074, China* **(liuruibei@hbou.edu.cn)**

(*Received 17 May 2023, Accepted 09 May 2025*)

***Corresponding author's email: zhangjinye@hbut.edu.cn**

सार – जैसे-जैसे भूमंडलीय उष्णता और प्रचंड मौसम की घटनाएँ लगातार बढ़ रही है, वायुमंडल में कार्बन डाइऑक्साइड (CO2) की सांद्रता दुनिया भर में एक बड़ी चिंता का विषय बन गई है। 2019 के अंत में शुरू हुई कोविड-19 महामारी के कारण मानवीय गतिविधियों पर महत्वपूर्ण प्रतिबंध लगे जिसके परिणामस्वरूप ग्रीनहाउस गैसों की सांद्रता में परिवर्तन हुआ। चीन के हुबेई में महामारी की पहली लहर के दौरान GOSAT उपग्रह से प्राप्त CO2 डेटा और COVID-19 डेटा का विश्लेषण किया गया। कोविड-19 महामारी के प्रकोप के दौरान CO2 सांद्रता में 1.54ppm की कमी आई जो पिछले वर्षों की तुलना में अभूतपूर्व गिरावट थी। हुबेई प्रांत में CO2 सांद्रता का कम मूल्य चीन के 34 प्रांतों में दूसरे स्थान पर रहा जो ताइवान प्रांत के बाद दूसरे स्थान पर है। प्रकोप के नियंत्रण में आने के बाद, CO2 सांद्रता धीरे-धीरे सामान्य स्तर पर लौट आई। निवासियों की आवाजाही और औद्योगिक उत्पादन पर प्रतिबंधों के कारण प्राथमिक, द्वितीयक और तृतीयक उद्योगों में बिजली की खपत में उल्लेखनीय गिरावट आई, जबकि आवासीय क्षेत्रों में बिजली की खपत में काफी वृद्धि हुई, जिसके परिणामस्वरूप आवासीय क्षेत्र से जीवाश्म CO2 उत्सर्जन में वृद्धि हुई। हालाँकि, बिजली उत्पादन, उद्योग, परिवहन, सार्वजनिक सेवाओं और विमानन से होने वाले उत्सर्जन में काफी कमी आई। जैसे-जैसे महामारी कम हुई, ये प्रवर्ति ठीक होने लगी।

इस अध्ययन में मीथेन (CH4) सांद्रता का भी विश्लेषण किया गया। फरवरी 2020 में CH4 की सांद्रता में 4.76 पीपीबी की कमी आई जो महामारी के दौरान सबसे बड़ी गिरावट और हुबेई में कोविड 19 प्रकोप के सबसे गंभीर चरण को दर्शाता है। इसके अलावा मार्च 2019 और मार्च 2021 (क्रमशः 1.21 और 1.06 पीपीबी) में मीथेन सांद्रता वृद्धि की तुलना में, मार्च 2020 में मीथेन सांद्रता में वृद्धि -0.23 पीपीबी थी, जो पिछले और बाद के वर्षों में देखी गई वृद्धि से कम थी। इसी तरह CH4 में भी काफी उतार-चढ़ाव देखा गया, जिसमें कोविड-19 संकट के चरम के दौरान सबसे बड़ी गिरावट देखी गई, जिसके बाद कोविड-19 महामारी की स्थिति में सुधार होने पर CH4 में भी सुधार हुआ।

ABSTRACT. As global warming intensifies and extreme weather events become more frequent, the concentration of carbon dioxide (CO_2) in the atmosphere has become a major concern worldwide. The COVID-19 pandemic, which began at the end of 2019, led to significant restrictions on human activities, resulting in changes of greenhouse gases' concentrations. CO_2 Data from GOSAT satellite and COVID-19 data during the first wave of the pandemic in Hubei, China, were analyzed.CO_2 concentration during the outbreak of COVID-19 decreased by 1.54 ppm, an unprecedented decline in previous years. The reduced value of the CO_2 concentration in Hubei province ranked second among the 34 provinces in China, only second to Taiwan province. After the outbreak was under control, CO_2 concentration gradually returned to normal levels. The restrictions on resident mobility and industrial production led to a significant drop in electricity consumption across the primary, secondary and tertiary industries, while residential electricity consumption increased substantially, resulting in a rise in fossil CO_2 emissions from the residential sector. However, emissions from power generation, industry, transport, public services, and aviation all significantly decreased. As the pandemic subsided, these trends began to recover.

Methane (CH_4) concentrations were also analyzed in this study. In February 2020, CH_4 concentration decreased by 4.76 ppb, marking the largest decline during the pandemic and reflecting the most severe stage of the outbreak in Hubei. Furthermore, compared to the methane concentration increments in March 2019 and March 2021 (1.21 and 1.06 ppb, respectively), the increment in methane concentration in March 2020 was -0.23 ppb, which was lower than the increments observed in the previous and following years. Similarly, CH_4 showed substantial fluctuations, with the largest drop observed during the peak of the COVID-19 crisis, followed by a recovery as the pandemic situation improved.

Key words – COVID-19, CO_2, CH_4, GOSAT, Hubei.

1. Introduction

Since the first case of COVID-19 was reported in Wuhan, Hubei Province, China, there were 632,533,408 confirmed cases of COVID-19 worldwide, including 6,592,320 deaths until 15 November 2022 (WHO, 2022). This brought much trouble to people's lives but also some positive effects. City residents with severe epidemics were passively or actively quarantined, significantly reducing human activities. As a result, commercial, industrial, and domestic emissions were reduced.

It is well known that the emission of CO_2 is one of the main drivers of climate change and global warming, and CH_4 is the second largest anthropogenic greenhouse gas after CO_2 (Houghton, 2009). Over 80% of fuel combustion-related CO_2 emissions can be attributed to electricity generation, transportation, and industrial operations (Quadrelli & Peterson, 2007). By the middle of June 2020, India witnessed a substantial decline in its daily fossil-based CO_2 emissions, experiencing a reduction of -11.6% (-5 to -25.7%) when compared to the average levels observed between 2017 and 2019. This resulted in an overall decrease in fossil-based CO_2 emissions of -139 (-62 to -230) $MtCO_2$ (Parida *et al.*, 2020). The presence of significant daily and seasonal fluctuations in local CO_2 levels hinders the prompt detection of a discernible signal (Dacre *et al.*, 2021). Therefore, localized blockades during the epidemic affected CO_2 emissions and regional CO_2 concentrations. The Chinese government responded quickly after the outbreak in Wuhan. Two temporary hospitals were built in ten days, and more than 38 thousand doctors and nurses from other provinces came to help Wuhan. The whole city was locked down. The life, commercial and industrial emissions were reduced during the lockdown. Thereby, CO_2 concentration was also reduced in the corresponding areas.

Several studies have documented a decline in CO_2/CH_4 emissions as a result of the worldwide implementation of lockdown measures (Moersen, 2020; Simpkins, 2020), while CH4 emissions have fluctuated, but the decline was not significant (Sharma, & Verma, 2021). This reduction in emissions can be attributed to the restrictions imposed during the global lockdown (Le Quéré *et al.*, 2020; Rugani & Caro, 2020). China, being among the top global emitters of greenhouse gases experienced a significant decrease of approximately 10% in greenhouse gas emissions by the end of March compared to the previous year due to the lockdown measures (Tollefson, 2020). Hwang's analysis did not provide evidence supporting a global decline in CO_2 concentration during the initial phase of the COVID-19 pandemic (Hwang *et al.*, 2021). Few studies have focused on the change of CO_2 concentrations under epidemic scenarios in individual provinces or cities.

In this study, we collected and analyzed COVID-19 data as well as CO_2 and CH_4 emissions data for China during the pandemic. We divided the time series of COVID-19 and CO_2 into six distinct stages and examined their spatial distribution across seven economic regions in the country. Additionally, we conducted a more in-depth analysis of the impact of COVID-19 on CO_2 emissions and electricity consumption in Hubei. Our findings provide insight into the short-term and long-term effects of the COVID-19 pandemic on CO_2 and CH_4 concentrations.

2. Data and methods

2.1. *Study area*

Hubei Province is in the central region of China and within the latitude of 29.031° N to 33.113° N and longitude of 108.362° E to 116.131° E. The province's geographical area is 185,900 km^2, with a total population of 58,300,000. Hubei Province is in the subtropical zone and most of the province has a humid subtropical monsoon climate except for the alpine climate in the high mountain area. COVID-19 was first reported in Hubei Province, Wuhan City, then spread rapidly in countries worldwide.

2.2. *Concentration data*

We use CO_2 as an example to present the concentration data. Regional lockdowns after the outbreak of the new crown epidemic. CO_2 emissions have changed across sectors in different countries. It will be reflected in the value of CO_2 concentration in each region.

CO_2 emission $\left(CO_2^{emi}\right)$ and CO_2 absorption $\left(CO_2^{abs}\right)$ can basically reflect the change of CO_2 concentration,

TABLE 1

Location (latitude and longitude), elevation (meters above sea level, masl), data used and correlation coefficient with GOSAT data for the 3 CO_2 ground-based observation sites used in this study

Site	Lat./Long.	Elevation (masl)	Data used	Correlation coefficient
Mt. Waliguan	36.29° N, 100.90° E	3810	June 2009 to December 2021	0.97**
Shangdianzi	40.65° N, 117.12° E	287	June 2009 to September 2015	0.64**
Lulin	23.47° N, 120.87° E	2862	June 2009 to December 2021	0.98**

**0.01 level (significantly correlated on both sides)

which is analyzed by the following linear model in this paper:

$$\Delta CO_2^{con} = \alpha \cdot CO_2^{emi} - \beta \cdot CO_2^{abs}$$

$\left(CO_2^{emi}\right)$ is a function of the confinement index (CI) for each day of the pandemic year 2020, which is estimated using the following equation:

$$\Delta CO_2^{emi}(c,s,d) = CO_2(c) \cdot \delta S(c) \cdot \Delta A[s, d(CI, c)]$$

where $CO_2^{emi}(c,s,d)$ is change in CO_2 emissions for each country (c), sector (s) and day (d).

Currently, two main ways to monitor CO_2 concentration are ground-based observation and remote sensing monitoring. The atmospheric background stations can provide long-term, stable and continuous global atmospheric concentration monitoring data. In the past decade, remote sensing technology has been developed rapidly, and remote sensing monitoring has become the primary method for monitoring the distribution of atmospheric CO_2. The US, Europe, and other countries have successfully launched satellites to monitor atmospheric CO_2 concentration, such as atmospheric infrared detector AIRS (Atmospheric InfraRed Sounder), OCO-2 (Orbital Carbon Observer 2), IASI (Infrared Atmospheric Sounding Interferometer), observation technology satellite GOSAT (Greenhouse Gases Observing Satellite) and carbon dioxide observation scientific experiment satellite TANSAT, etc. Among the various missions, GOSAT and OCO-2 hold significant importance. OCO-2, initiated in 2014, represents the inaugural venture of the United States National Aeronautics and Space Administration (NASA) focused on measuring atmospheric CO_2 concentration (Fei Jiang *et al.*, 2022). The launch of GOSAT in 2009 by Japan established it as the principal satellite for greenhouse gas monitoring. The GOSAT satellite incorporates the utilization of the Fourier Transform Spectrometer (FTS) and the Cloud and Aerosol Imager (CAI). FTS is employed for detecting greenhouse gases, while CAI synchronizes the collection of cloud and aerosol information (Shanshan *et al.*, 2013). GOSAT Level 3 products have been available from June 2009, and the Level 3 products from January 2010 to December 2021 are collected and used in this paper. GOSAT Level 3 products have published uncorrected and corrected versions of the data. The uncorrected version is raw data obtained from satellites. The raw data is corrected with the method of outlier-corrected and kriging-interpolated to make the corrected version. The spatial resolution of the corrected version is 2.5° × 2.5°. The corrected version data are interpolated by further Kriging method in this paper and the interpolated data have a higher spatial resolution of 1° × 1°. The monthly CO_2 concentration of the target area can be obtained according to its latitude and longitude coordinates.

Table 1 demonstrates that the World Data Center for Greenhouse Gases (WDCGG) offers ground-based observation data from stations such as Mt. Waliguan (WLG), Shangdianzi (SDZ), and Lulin (LLN) (Zhang, & Zhang, 2018). The CO_2 products derived from GOSAT and the ground-based observations exhibit strong agreement, with correlation coefficients of 0.97 (WLG), 0.64 (SDZ), and 0.98 (LLN), passing a significance test at a 0.01 level.

Fig. 1 shows the comparison of ground-based observations data with GOSAT CO_2 data. Figs. 1(a1) and 1(a2) show the comparison of the WLG Station with the GOSAT by line chart and violin chart of CO_2 concentration data. The data used is from June 2009 to December 2021. The line chart shows that WLG and GOSAT data have good consistency. Moreover, the values of WLG data are overall higher than GOSAT's. The violin chart represents the one-quarter median, the median, and the three-quarter median of WLG data are slightly higher than those of GOSAT. Furthermore, the distribution of WLG data is more discrete than GOSAT's. Figs. 1(b1) and 1(b2) show the comparison of SDZ Station with

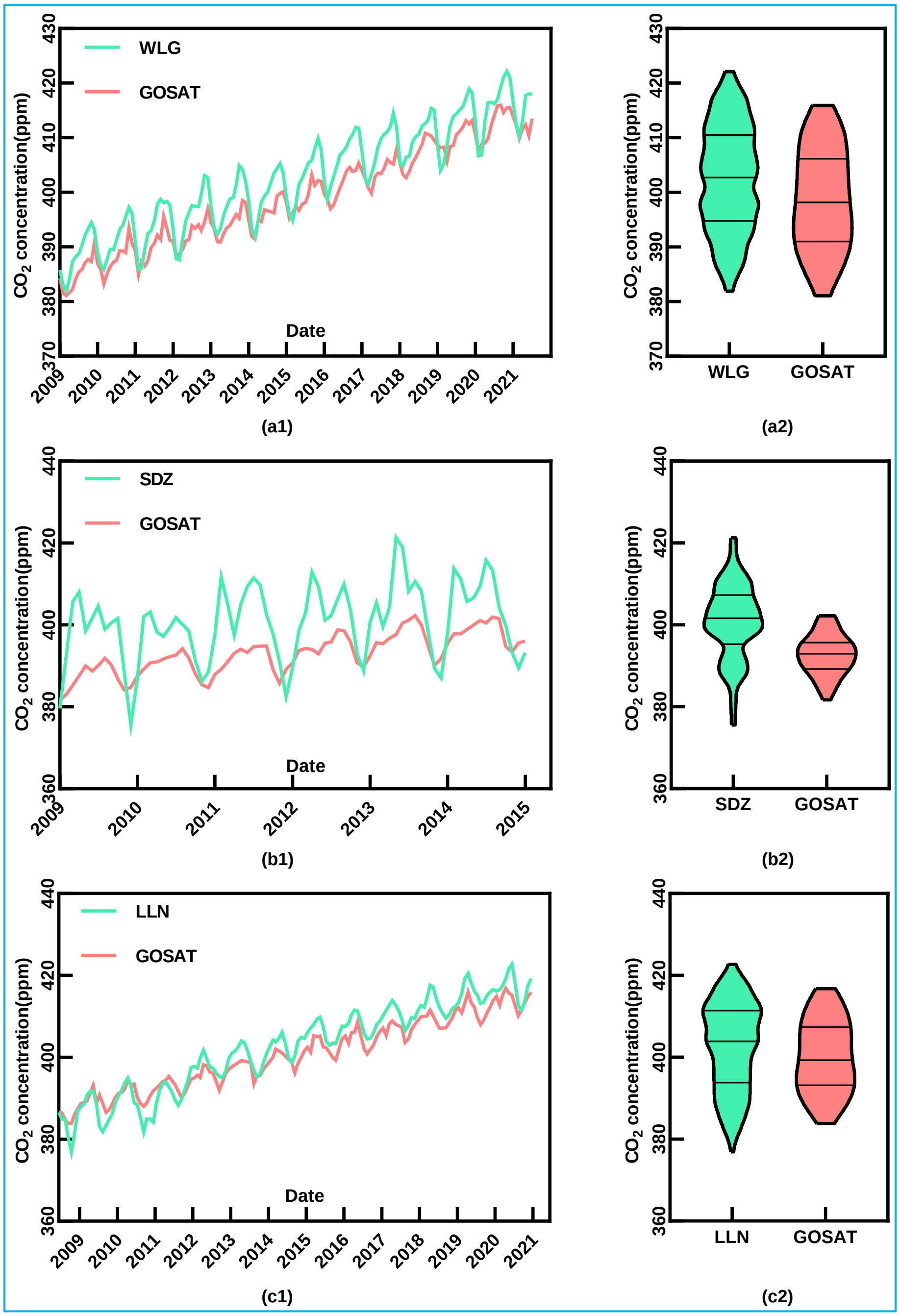

Fig. 1. Comparison of ground-based observations data with GOSAT CO_2 data.**a1** Comparison of WLG Station with GOSAT by line chart of CO_2 concentration data, **a2** Comparison of WLG Station with GOSAT by violin chart of CO_2 concentration data, **b1** Comparison of SDZ Station with GOSAT by line chart of CO_2 concentration data, **b2** Comparison of SDZ Station with GOSAT by violin chart of CO_2 concentration data, **c1** Comparison of LLN with GOSAT by line chart of CO_2 concentration data, **c2** Comparison of LLN Station with GOSAT by violin chart of CO_2 concentration data

GOSAT by line chart and violin chart of CO_2 concentration data. The data used is from June 2009 to September 2015. The comparative characteristics of SDZ data are similar to those of WLG, but the correlation is relatively worse. Fig. 1(c1) and Fig. 1(c2) show the comparison of LLN Station with GOSAT by line chart

TABLE 2

Timeline of COVID-19 responses in Hubei

Phase	Time	Action
Phase 1	Before January 2020	The epidemic has not been detected
Phase 2	January 2020	Timely and decisive action was taken
Phase 3	February 2020	The initial efforts showed positive results.
Phase 4	March 2020	Newly confirmed domestic cases reduced to single digits
Phase 5	April 2020	An early triumph achieved in the crucial battle at hand
Phase 6	After April 2020	Ongoing prevention and control

and violin chart of CO_2 concentration data. The data used is from June 2009 to December 2021. The comparative characteristics of LLN data are similar to those of WLG.

According to the above, all the CO_2 data show a strong correlation and apparent periodicity. Moreover, all the ground-based observations data tend to be generally more prominent than GOSAT data.

2.3. *COVID-19 data*

Hubei's fight against COVID-19 can be divided into six phases (SCIO, 2020). Before 27 December 2019 is Phase 1 without epidemic detected. From 27 December, 2019 to 19 January, 2020 is Phase 2 for a swift response to the public health emergency. At this time, the epidemic began to spread, and production and life began to be affected to a certain extent. From 20 January to 20 February 2020 is Phase 3 for initial progress in containing the virus, and it is also the phase of total lockdown. At this time, residents were blocked at home, and transportation and factory production were stopped entirely. From 21 February to 17 March, 2020 is Phase 4 for newly confirmed domestic cases dropping to single digits on the Chinese mainland, and it is also the phase of effective containment of the epidemic. From 18 March to 28 April, 2020 is Phase 5 for an initial victory in the critical battle in Wuhan. At this time, production and life began to resume gradually. 29 April, 2020 is Phase 6 for ongoing prevention and control. At this time, residents' life and social production have returned to normal. As shown in Table 2, a timeline of COVID-19 responses in Hubei is divided into six monthly phases to facilitate the comparative study of various factors.

The release of case data in the early stages of the COVID-19 outbreak was messy. This paper uses Python to obtain case data during the first wave of the epidemic in China from NetEase, the National Health Commission of the People's Republic of China and the official websites of Chinese provinces. These data were used in the analysis of changes in CO_2 concentration.

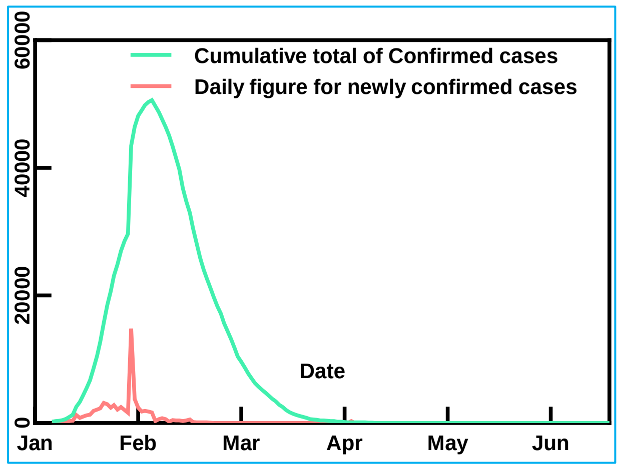

Fig. 2. Cumulative total of confirmed cases and daily figure for newly confirmed cases over Hubei

2.4. *Other data*

We obtained the daily CO_2 emissions data from the Global Carbon Project (GCP), available at https://www.icos-cp.eu/gcp-covid19. The mean daily CO_2 emissions of Hubei Province for 2017-2020 were available from the GCP, which utilized daily energy usage data of POSOCO. Moreover, the detailed parameters used in this methodology can be seen from the GCP. The sectors (power, industry, surface transport, public sector, residential and aviation) change of CO_2 emissions data were also employed to assess the impacts of restrictive confinement measures on Hubei's CO_2 emissions.

The Hubei Provincial Bureau of Statistics (HPBS) organizes and implements statistical surveys on the province's primary energy and resource utilization conditions. It collects, collates, and presents statistics on surveys. This paper obtained the electricity consumption data for 2019 and 2020 released by the HPBS. Monthly electricity consumption data were collated. Electricity consumption includes primary industry consumption, secondary industry consumption, tertiary industry consumption and domestic electricity consumption. The

TABLE 3

The monthly average CO_2 concentration in Hubei from 2010 to 2021

Year	CO_2 Concentration (ppm)											
	Jan	Feb	Mar	Apr	May	Jun	Jul	Aug	Sep	Oct	Nov	Dec
2010	392.10	391.35	392.21	393.10	392.72	388.81	**	**	386.51	390.49	392.12	391.62
2011	395.98	395.63	395.96	393.66	391.42	388.83	**	385.73	387.58	388.81	392.85	393.89
2012	395.37	397.24	398.23	396.02	394.06	391.90	390.65	388.00	390.77	392.40	394.99	396.63
2013	398.43	397.13	401.35	400.24	399.86	397.41	**	395.16	392.21	395.43	397.92	397.98
2014	400.67	401.90	399.32	400.95	400.62	396.65	392.30	392.01	394.81	397.60	399.64	*
2015	*	403.74	402.40	403.04	402.02	**	395.11	394.75	396.97	400.12	402.11	403.03
2016	406.64	405.43	405.10	405.27	405.53	400.33	**	398.42	399.38	402.92	406.28	406.11
2017	407.86	407.20	410.32	408.96	407.02	404.44	**	**	402.79	406.58	408.09	409.80
2018	409.41	410.44	411.32	410.87	409.23	408.14	406.79	402.90	405.63	407.29	408.74	*
2019	412.01	412.42	412.66	412.62	413.39	410.15	407.74	406.24	407.61	410.93	412.50	412.32
2020	415.57	414.04	416.84	414.99	414.77	414.28	**	409.82	410.22	413.92	414.20	417.30
2021	417.62	417.13	419.41	417.33	417.43	416.89	**	411.22	414.19	414.28	416.23	418.48

* products were not available, ** data is vacant

consumption of the transportation sector is part of the consumption of the tertiary industry.

3. Results and discussion

3.1. *Time series analysis of XCO_2/XCH_4 and COVID-19 in Hubei*

Fig. 2 shows the cumulative total of confirmed cases and the daily figure for newly confirmed cases in Hubei. The cumulative total confirmed cases increased rapidly in Phase 2, increased more steeply in Phase 3, was controlled and rapidly decreased in Phase 4 and Phase 5 and was cleared to zero in Phase 6. The daily figure for newly confirmed cases increased steadily in Phase 2, declined at the end of Phase 2, rose steeply in Phase 3, fell sharply, and was almost always zero in Phase 4, Phase 5 and Phase 6. On 18 February 2020 (during Phase 3), the cumulative total confirmed cases reached the maximum of 50633 in Hubei. Furthermore, on 12 February 2020 (during Phase 3), the daily figure for newly confirmed cases peaked at 14840 in Hubei.

Table 3 shows Hubei's monthly average CO2 concentration from 2010 to 2021. From January 2010 to December 2021, the GOSAT data products were unavailable for three months and vacant in Hubei for ten months. Data indicated that the CO_2 concentration over Hubei in January 2010 was only 392.10 ppm and increased to 418.48 ppm in December 2021. During the 12 years, the CO_2 concentration increased by 26.38 ppm (about 2.20 ppm/year) in Hubei. The CO_2 concentration in China has apparent seasonal variation, with the lowest CO_2 concentration in summer and the highest in spring, with an annual increase of about two ppm. CO_2 concentration in Hubei Province also varies seasonally. The CO_2 concentration in autumn and winter is higher than in spring and summer, with the largest in March and April and the smallest in July and August. In the case of seasonal changes, it is not easy to draw intuitive conclusions just by observing the CO_2 concentration. Therefore, detrended CO_2 concentration was considered to observe CO_2 changes. The detrended carbon dioxide concentration is the monthly increment of CO_2 concentration. The change in CO_2 concentration in Hubei Province in each month compared with the previous month can be seen in Table 3. The CO_2 concentration increased in March, September, November and December. Concentrations decreased in January, February, April, May, June, July and August.

Five bar graphs in Fig. 3 show the monthly increments of CO_2 concentration in Hubei Province from 2010 to 2020. The abscissa in the figure is the year and the ordinate is the monthly increment in CO_2 concentration (unit : ppm). Fig. 3(a) shows the increment from December of the previous year to January (excluding 2015 and 2019). From December 2019 to January 2020, the

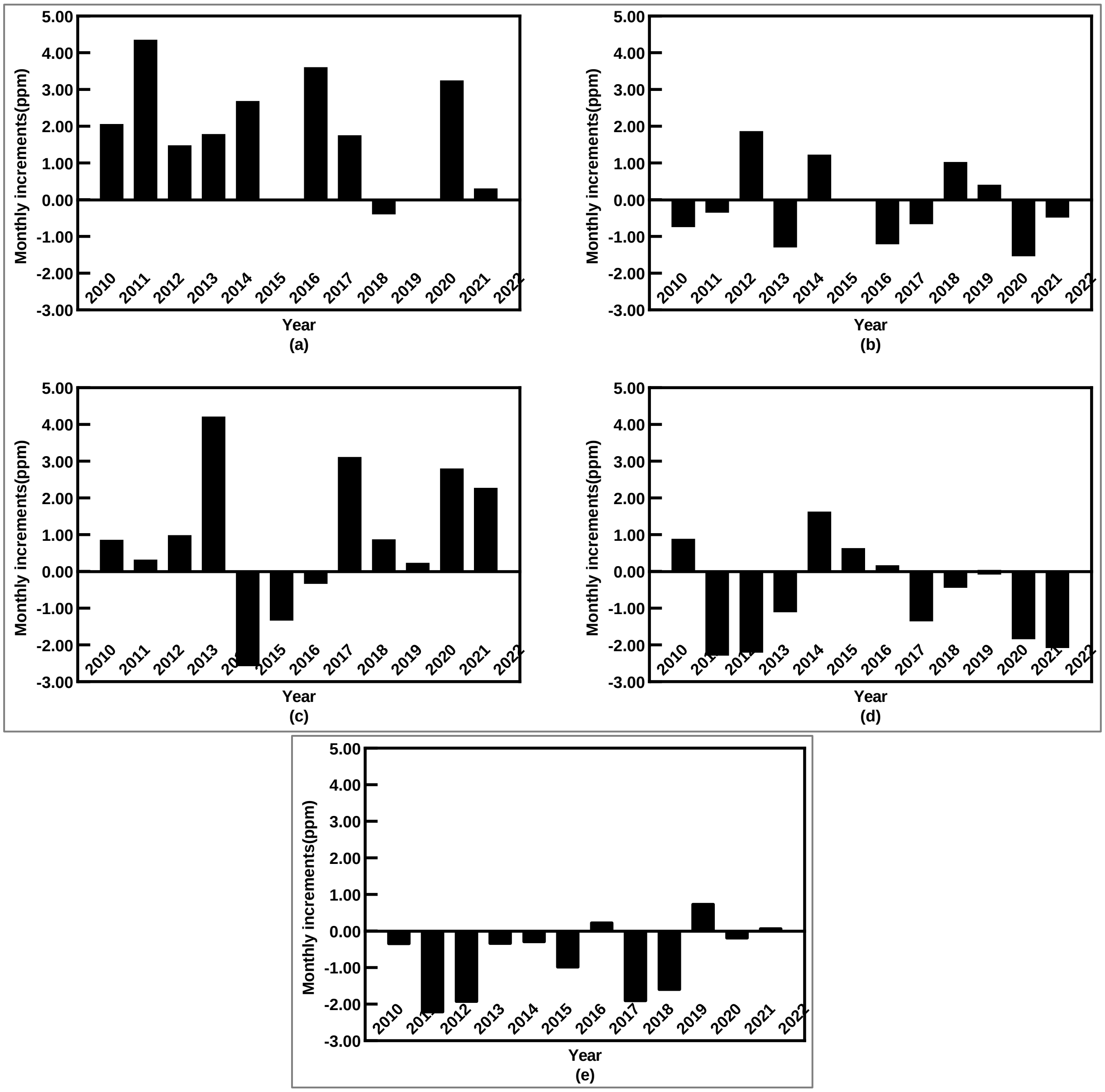

Figs. 3(a-e). The monthly increments of CO_2 concentration of Hubei Province from 2010 to 2020: from December of the previous year to January (excluding 2015 and 2019) (a); from January to February(excluding 2015) (b); from February to March (c); from March to April (d); from April to May (e)

CO_2 concentration increased by 3.25ppm, which is second to 4.36ppm in 2011 and 3.61ppm in 2016. Fig. 3(b) shows the increment from January to February (excluding 2015). The decline of CO_2 concentration exceeded 1.54ppm for the first time in 2020 compared to previous years. From January to February 2020, Hubei was during Phases 2 and 3 with the most severe epidemic among epidemics and its CO_2 changes also showed differences from previous years. Fig. 3(c) shows the increment from February to March. CO_2 concentrations increased by 2.8 ppm in 2020, lower than 4.22 ppm in 2013 and 3.12 ppm in 2017. Figs. 3(d&e) show the increments from March to April and April to May. CO_2 concentrations increased by -1.84 ppm from March to April 2020 and -0.23 ppm from April to May 2020.

Table 4 shows Hubei's monthly average CH_4 concentration from 2010 to 2021. From January 2010 to

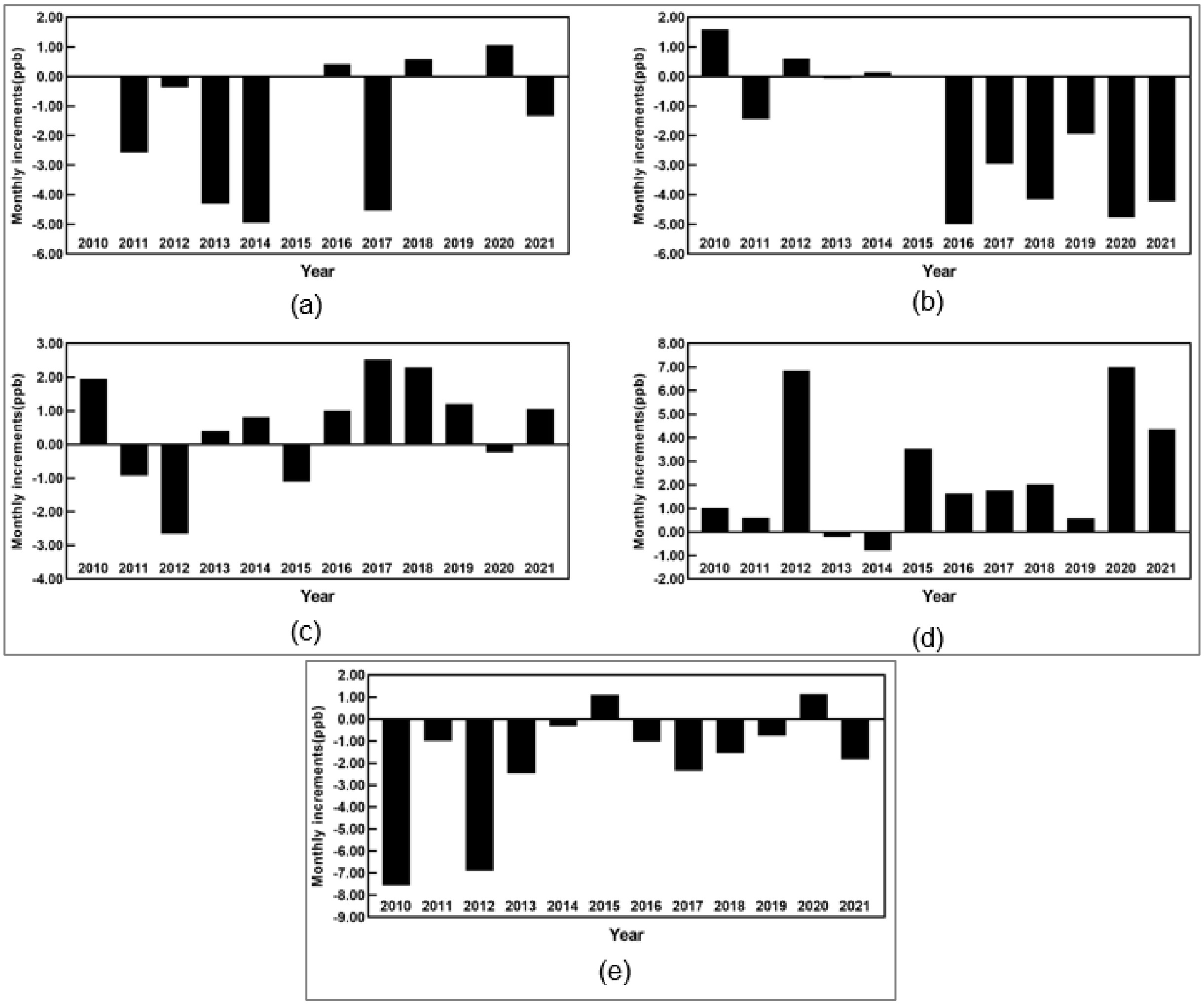

Figs. 4(a-e). The monthly increments of CH_4 concentration of Hubei Province from 2010 to 2020: from December of the previous year to January (excluding 2010, 2015 and 2019) (a); from January to February (excluding 2015) (b); from February to March (c); from March to April (d); from April to May (e)

TABLE 4

The monthly average CH_4 concentration in Hubei from 2010 to 2021

Year	CH_4 Concentration (ppb)											
	Jan	Feb	Mar	Apr	May	Jun	Jul	Aug	Sep	Oct	Nov	Dec
2010	1784.16	1785.74	1787.69	1788.71	1781.15	1776.35	1775.90	1782.01	1787.83	1798.09	1794.74	1793.08
2011	1790.49	1789.05	1788.13	1788.72	1787.71	1779.18	1776.16	1783.67	1792.93	1796.10	1797.94	1793.15
2012	1792.78	1793.38	1790.73	1797.59	1790.71	1784.43	1783.83	1789.80	1798.53	1806.33	1808.61	1806.48
2013	1802.18	1802.21	1802.61	1802.41	1799.96	1791.01	1791.70	1800.03	1809.66	1814.97	1814.02	1813.58
2014	1808.64	1808.77	1809.59	1808.81	1808.49	1799.47	1800.29	1807.49	1819.76	1823.82	1822.24	**
2015	**	1813.38	1812.28	1815.82	1816.92	1809.86	1809.37	1816.21	1824.75	1833.56	1829.75	1830.43
2016	1830.86	1825.88	1826.88	1828.52	1827.48	1821.66	1818.01	1824.84	1834.95	1842.38	1843.62	1837.95
2017	1833.42	1830.47	1833.00	1834.78	1832.43	1826.29	1825.62	1831.48	1843.25	1851.29	1842.71	1842.48
2018	1843.06	1838.91	1841.19	1843.21	1841.68	1838.38	1837.35	1841.63	1851.01	1862.02	1856.87	**
2019	1851.09	1849.16	1850.37	1850.94	1850.19	1848.28	1846.26	1849.66	1859.65	1864.48	1865.57	1858.69
2020	1859.76	1854.99	1854.77	1861.76	1862.90	1855.81	1852.08	1863.63	1873.70	1880.61	1878.25	1878.46
2021	1877.13	1872.91	1873.97	1878.33	1876.51	1870.60	1872.97	1877.53	1891.91	1898.69	1899.88	1889.83

* products were not available, ** data is vacant

TABLE 5

Seven geographic regions in China and provinces included

Region	Provinces included
North China	Beijing, Tianjin, Hebei, Shanxi, and InnerMongolia
Northeast China	Liaoning, Jilin and Heilongjiang
East China	Shanghai, Jiangsu, Shandong, Zhejiang, Anhui, Jiangxi Fujian and Taiwan
Central China	Henan, Hubei and Hunan
South China	Hong Kong, Macau,Hainan, Guangdong and Guangxi
Southwest China	Sichuan, Yunnan, Guizhou, Tibet and Chongqing
Northwest China	Shaanxi, Gansu, Qinghai, Ningxia, and Xinjiang

December 2021, the GOSAT data products were unavailable for three months and vacant in Hubei for ten months. Data indicated that the CH_4 concentration over Hubei in January 2010 was 1784.16 ppb and increased to 1889.83 ppb in December 2021. During these 12 years, the CH_4 concentration increased by 105.67 ppb (approximately 8.81 ppb/year). The CH_4 concentration in Hubei shows apparent seasonal variation, with the lowest concentrations in summer (June, July and August) and the highest in autumn and winter (November and December). The concentration increased in March, September, November, and December, and decreased in January, February, April, May, June, July and August.

The five bar graphs in Fig. 4 show the monthly increments of CH_4 concentration in Hubei Province from 2010 to 2021. The abscissa in the figure represents the year and the ordinate represents the monthly increment in methane concentration (unit: ppb). Fig. 4(a) shows the increment from December of the previous year to January (excluding data from 2010, 2015, and 2019). Fig. 4(b) displays the increment from January to February (excluding data from 2015). In February 2020, methane concentration decreased by 4.76 ppb, which is the largest decline for this period, reflecting the most severe phase of the epidemic in Hubei. Fig. 4(c) shows the increment from February to March. Compared to the methane concentration increments in March 2019 and March 2021 (1.21 and 1.06 ppb, respectively), the increment in methane concentration in March 2020 was -0.23 ppb, which was lower than the increments observed in the previous and following years. Figs. 4(d&e) show the increments from March to April and April to May. From March to April 2017, methane concentration decreased by 2.35 ppb, while from April to May 2020, it increased by 1.13 ppb, showcasing the rapid recovery of social production and transportation after the stabilization of the COVID-19 pandemic.

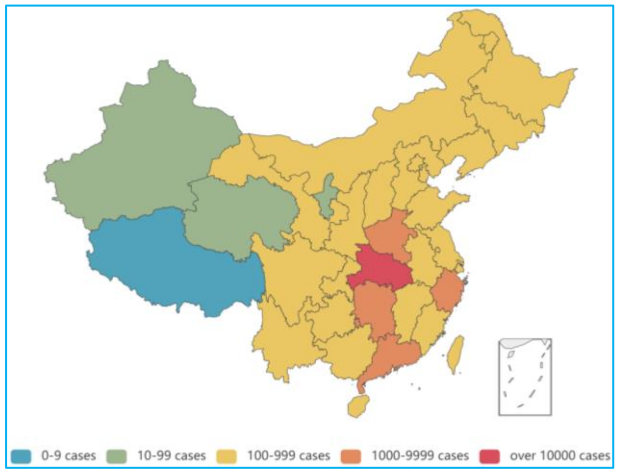

Fig. 5. Spatial distribution of cumulative confirmed cases in 34 provinces in China on 1 July, 2020

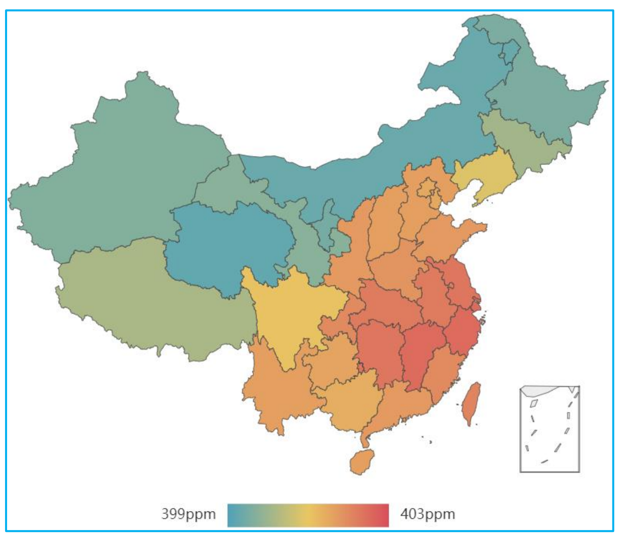

Fig. 6. Spatial distribution of average CO_2 concentration in China from 2010 to 2021

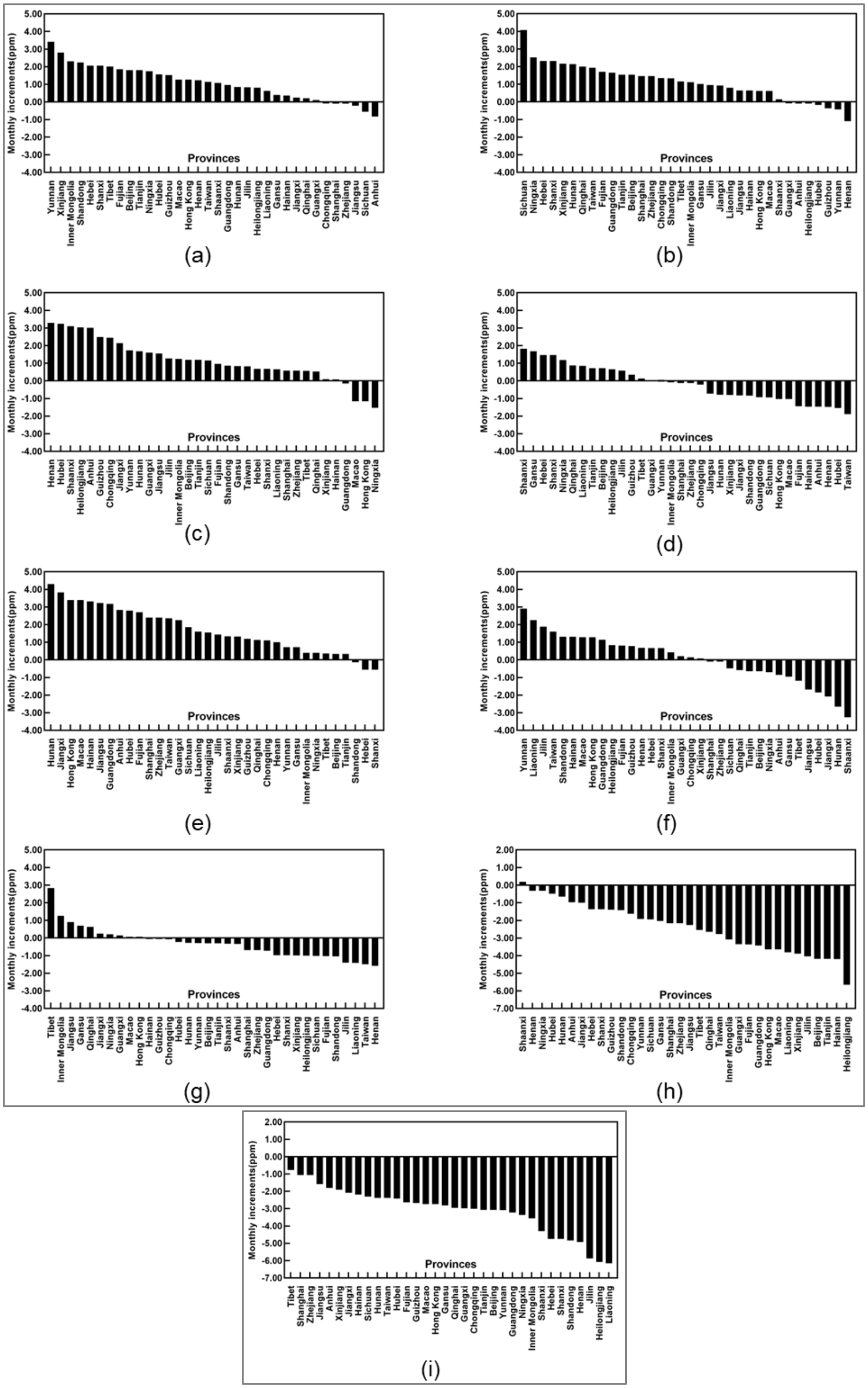

Figs. 7(a-i). Shows the monthly increments of CO_2 concentration in 34 provinces in 2020

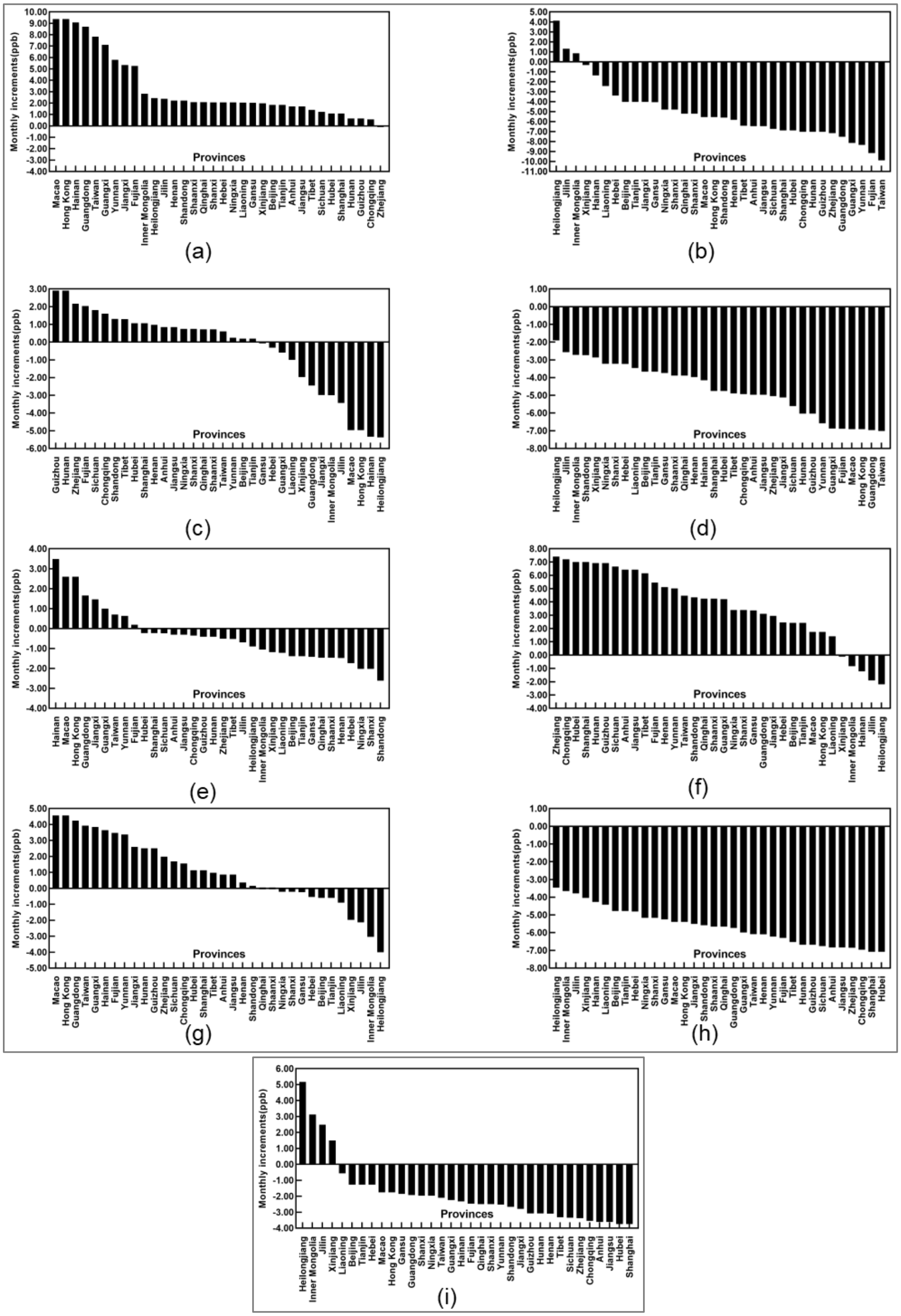

Figs. 8(a-i). The monthly increments of CH_4 concentration of 34 provinces in 2020: from October to November (a); from November to December (b); from December of the previous year to January (c); from January to February (d); from February to March (e); from March to April (f); from April to May (g); from May to June (h); from June to July (i)

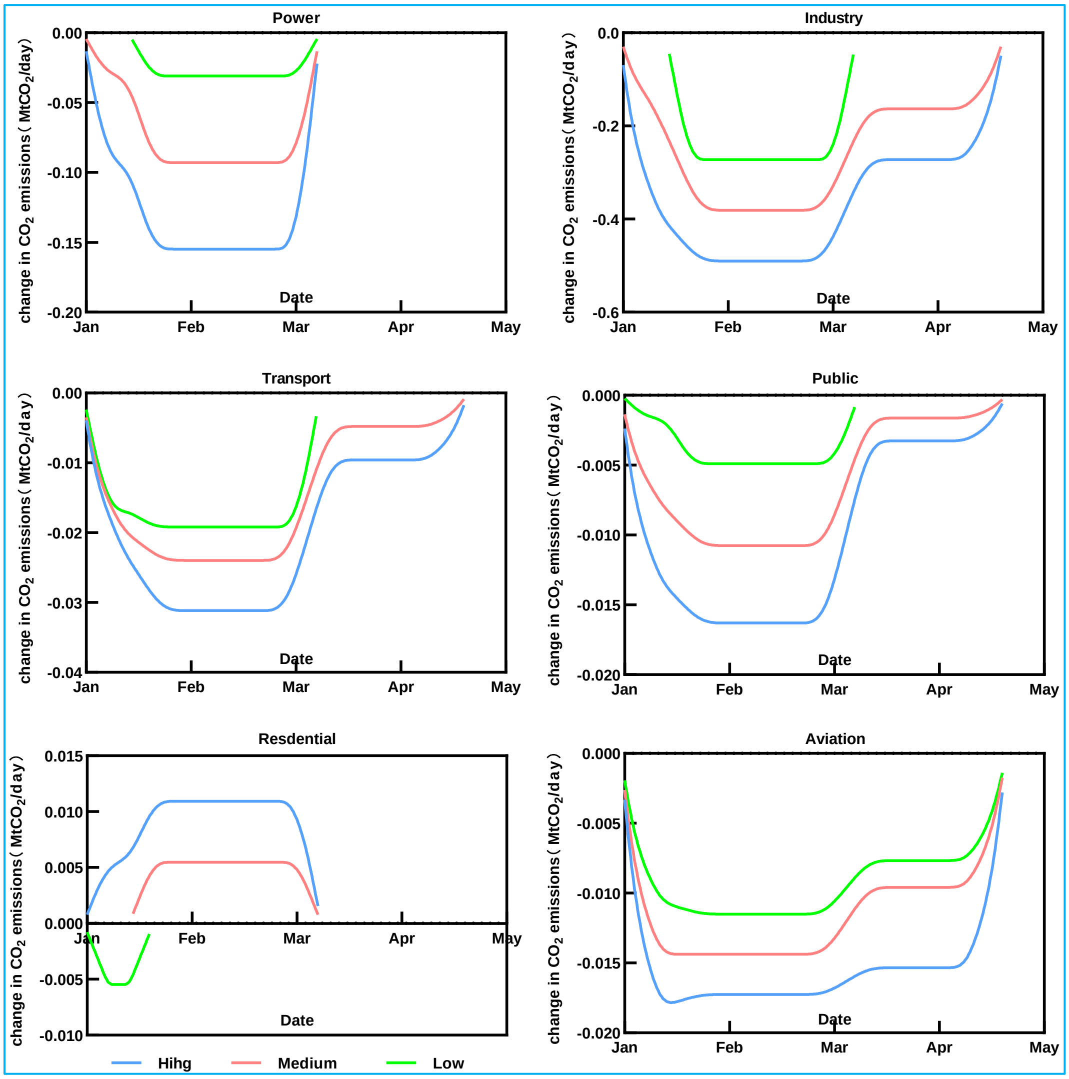

Fig. 9. Sector-wise change in daily fossil CO_2 emissions ($MtCO_2$/day) during COVID-19 with smooth function

3.2. *Spatial distribution of XCO_2/CH_4 and COVID-19 in China*

China is a vast country containing 34 provinces. As shown in Table 5, China can be divided into seven geographical regions : North China (NC), Northeast China (NEC), East China (EC), Central China (CC), South China (SC), Southwest China (SWC) and Northwest China (NWC).

Fig. 5 shows the spatial distribution of cumulative confirmed cases in 34 provinces in China on 1 July, 2020. 68,135 cases confirmed in Hubei Province, far more than in other provinces. No other provinces have confirmed more than 1,642 cases. Hubei province is the epicenter of the outbreak. From a national perspective, the most severely affected areas are CC, EC and SC, followed by NEC, SWC and NC. Furthermore, NWC is the least affected by the epidemic.

CO_2 concentration in China was low in NWC and high in SEC. Human activities influence this phenomenon. Fig. 6 shows the spatial distribution of average CO_2 concentration in China from 2010 to 2021. There are apparent differences between different regions. The areas with the highest CO_2 concentrations are mainly CC, EC, and SC, followed by NEC, SWC and NC. Moreover, NWC has the lowest value.

Fig. 7 shows the monthly increments of CO2 concentration in 34 provinces in 2020, covering data from before, during, and after the pandemic. Fig. 7(a) displays

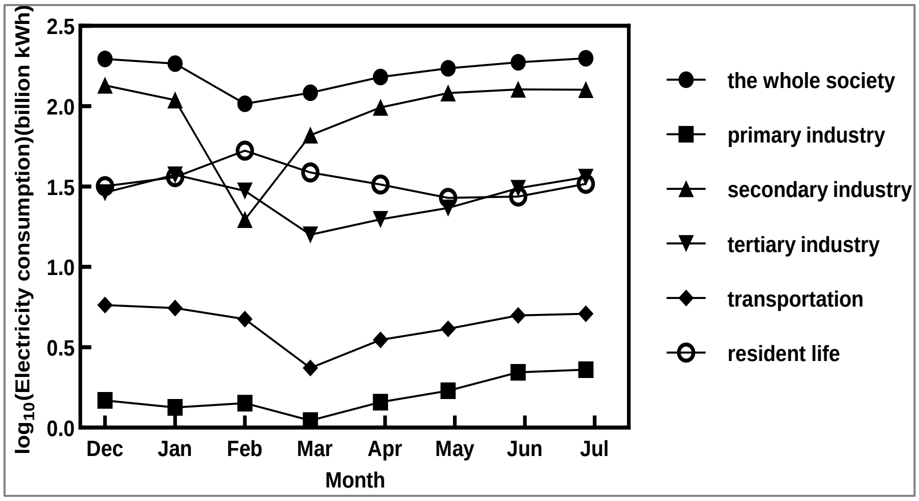

Fig. 10. Monthly electricity consumption in Hubei during COVID-19(billion kWh).The ordinate is the logarithm to base 10 of electricity consumption

the increment from October to November 2019, where Hubei's CO2 concentration increased by 1.57 ppm, ranking 12th in the country. Fig. 7(b) shows the increment from November to December 2019, where Hubei's CO2 concentration decreased by -0.18 ppm, ranking 31st. Except for the November to December period, Hubei's CO_2 concentration increment from October to November 2019 ranked in the upper-middle level nationally. During the pandemic, Fig. 7(c) shows the increment from December 2019 to January 2020, where Hubei's CO_2 concentration increased by 3.25 ppm, ranking second nationally, just behind Henan. Fig. 7(d) displays the increment from January to February, where Hubei's CO_2 concentration decreased by -1.54 ppm, with the second-largest decrease, just after Taiwan. This period corresponds to the most severe phase of the pandemic, with lockdown measures halting production and transportation. Figs. 7(e-g) show the increments from February to March, March to April and April to May, respectively. Hubei's CO_2 concentration increased by 2.8 ppm from February to March, but then decreased by -1.84 ppm from March to April and -0.23 ppm from April to May, with national rankings of 9th, 31st and 14th, respectively, indicating mid-level to upper-middle performance. This period marks the initial easing of the pandemic. As the pandemic continued to ease, Fig. 7(h) shows the increment from May to June, where Hubei's CO_2 concentration decreased by -0.49 ppm, ranking 4th in the country. Fig. 7(i) shows the increment from June to July, where Hubei's CO_2 concentration decreased by -2.42 ppm, ranking 12th. In summary, before the pandemic, Hubei's CO_2 concentration increment ranked in the upper-middle level nationally. During the most severe phase (December 2019 to February 2020), Hubei's increment dropped sharply. However, as the pandemic eased, Hubei's CO_2 concentration increment gradually returned to the upper-middle level, particularly in May-June and June-July, where the increment decreased and ranked 4th and 12th, respectively, reflecting the gradual economic recovery after the pandemic.

Fig. 8 presents the monthly CH_4 concentration increment data for 34 provinces from October 2019 to July 2020. Fig. 8(a) shows the increment from October to November 2019, with Hubei Province's CH_4 concentration increasing by 1.09 ppb, ranking 29th nationwide. Fig. 8(b) shows the increment from November to December 2019, with Hubei Province's CH_4 concentration decreasing by -6.88 ppb, ranking 25th nationwide. Fig. 8(c) displays the increment from December 2019 to January 2020, with Hubei Province's CH4 concentration increasing by 1.06 ppb, ranking 9th nationwide. Fig. 8(d) shows the increment from January to February 2020, with Hubei Province's CH_4 concentration decreasing by -4.76 ppb, ranking 18th nationwide. Fig. 8(e) presents the increment from February to March 2020, with Hubei Province's CH_4 concentration decreasing by -0.23 ppb, ranking 10th nationwide. Fig. 8(f) displays the increment from March to April 2020, with Hubei Province's CH_4 concentration increasing by 7.00 ppb, ranking 3rd nationwide. Fig. 8(g) shows the increment from April to May 2020, with Hubei Province's CH_4 concentration increasing by 1.13 ppb, ranking 15th nationwide. Fig. 8(h) presents the increment from May to June 2020, with Hubei Province's CH_4 concentration decreasing by -7.08 ppb, ranking 34th nationwide. Fig. 8(i) shows the increment from June to July 2020, with Hubei Province's CH_4 concentration decreasing by -3.74 ppb, ranking 33rd nationwide.

Although the lockdown during the COVID-19 pandemic led to the suspension of some economic activities in Hubei Province, methane emissions are mainly influenced by long-term and persistent sources such as agriculture, waste management, and sewage treatment. At the beginning of the lockdown, these sources did not completely cease and some changes in social activities (such as logistics and household activities) could have contributed to the methane increment. In particular, the persistent emissions from wetland ecosystems, agricultural activities, landfills, and sewage treatment caused the methane increment to remain relatively high during the early stages of the pandemic.

3.3. *Changes in CO_2 emissions and electricity consumption in Hubei*

Fig. 9 showcases the sector-wise change in daily fossil CO_2 emissions (Mt CO_2/day) for the power, industry, transport, public, residential and aviation sectors. The results reveal a decrease in daily fossil CO_2 emissions across all sectors except the residential sector. The median lines indicate that all sectors' most significant daily fossil CO_2 emissions reduction occurred in February and March. As lockdown measures were relaxed and businesses resumed operations (excluding residential), the daily fossil CO_2 emissions started to recover from April.

Fig. 10 illustrates the monthly electricity consumption in Hubei during the COVID-19 pandemic. The y-axis displays the logarithmic consumption representation (base 10) to account for the significant differences in electricity consumption across regions. The results indicate a general decrease in overall consumption in January, followed by a significant drop in February. Starting from March, the consumption increased, eventually returning to normal by April. This trend was observed across the primary, secondary and tertiary industries, with the tertiary industry exhibiting the most pronounced decline due to its reliance on human activities.

On the other hand, the primary sector showed the most negligible impact due to its lower dependence on human activities. The transportation sector saw the most significant decrease in consumption in March, which can be attributed to the relocation of workforce and resources from other regions and the construction of makeshift hospitals. Conversely, residential electricity consumption increased in January, peaked in February, and started to decline in March before returning to normal levels by April. This can be linked to the lockdown measures implemented, resulting in residents staying home.

In terms of CO_2 emissions across different sectors and industries, the analysis before and after the pandemic shows clear patterns. During the lockdown phase from January to March, production and transportation activities came to a halt, resulting in a significant reduction in emissions. However, due to the stay-at-home measures, residential CO_2 emissions saw a sharp increase as people spent more time indoors. From March to April, as the pandemic was under control, production and transportation gradually resumed, leading to a partial recovery in carbon emissions. By May, as both residential and industrial activities returned to normal, CO_2 emissions stabilized, reflecting the resumption of daily life and economic activities.

4. Conclusions

In this study, we analyzed the time series of CO_2 concentration in Hubei and the spatial distribution of CO_2 concentration all over China. During the COVID-19 pandemic Phase 2, the CO_2 concentration increased by 3.25 ppm. It is second only to 3.29 ppm in Henan. Furthermore, it was second to 4.36 ppm in 2011 and 3.61 ppm in 2016. Referring to the increase in CO_2 concentration before the epidemic, the CO_2 concentration in Phase 2 increased significantly. During Phase 3, CO_2 concentration fell by 1.54 ppm in Hubei Province, ranking second. It fell by more than 1.5 ppm for the first time compared to previous years. Affected by the lockdown, the concentration in Phase 3 decreased significantly. During Phase 4, CO_2 concentration increased by 2.8 ppm, ranking 9th in the country. Moreover, it was lower than 4.22 ppm in 2013 and 3.12 ppm in 2017. After the outbreak began to be under control, the CO_2 concentration in Phase 4 increased. During Phase 5, CO_2 concentrations increased by -1.84 ppm, its decrement ranking 4th in the country. Furthermore, compared to previous years, its decrement also ranked fourth. After the epidemic was controlled, the CO_2 concentration in Phase 5 also returned to normal. During Phase 6, CO_2 concentrations decreased by 0.23 ppm, ranking 14th by increments. During periods of normalization, it is entirely at an average level.

After the onset of the COVID-19 pandemic, methane (CH4) concentration in Hubei province dropped significantly in February 2020, decreasing by 4.76 ppb, marking the largest decline during this period. This decline reflects the most severe phase of the outbreak in Hubei, when social and industrial activities were heavily restricted, leading to a sharp reduction in methane emissions. Compared to the methane concentration increments observed in March 2019 and March 2021 (1.21

ppb and 1.06 ppb, respectively), the methane increment in March 2020 was -0.23 ppb, much lower than the increments observed in the previous and following years, indicating the substantial impact of the pandemic's early stages on methane emissions. However, from April to May 2020, methane concentration increased by 1.13 ppb, showing a recovery trend as the pandemic began to stabilize and social production and transportation activities gradually restarted.

From the perspective of the 6 phases of developing the epidemic in China, the most apparent change in CO_2 concentration is Phase 3, followed by Phase 2. Phase 2 was a period of rapidly increasing CO_2 concentrations before the outbreak. Phase 3 is the most quickly developing stage of the epidemic. The CO_2 concentration in Phase 3 decreased. Phases 4, 5 and 6 changes have almost no apparent characteristics. It can be explained by changes in CO_2 emissions and electricity consumption in Hubei. During the lockdown, residents stayed home, industrial production reached a standstill, and transportation significantly shifted. The power consumption of the primary, secondary, and tertiary industries was significantly lower than usual from January to March, while residents' electricity consumption was significantly higher than normal levels from January to March. However, residential electricity consumption accounts for the most minor proportion of total electricity consumption in society. Therefore, except for the residential sector, the fossil consumption of power, industry, transport, public and aviation sectors dropped sharply in February and March, as did CO_2 emissions. Furthermore, the CO_2 concentration decreased in the second and third phases when the epidemic was severe.

In the short term of the concentrated outbreak of COVID-19, the CO_2 concentration in Hubei Province showed a particular downward trend. However, CO_2 emissions from local life, commerce, and industry recovered quickly after COVID-19 was under control, and this decreasing trend disappeared. Therefore, COVID-19 has little effect on CO_2 concentrations in the long term. In conclusion, this study provides evidence of the impact of reduced human activities on CO_2 emissions, as seen in Hubei Province during the first round of the COVID-19 pandemic. The results suggest that reducing human activities in transportation and industry may be the most effective way to reduce CO_2 emissions. The trajectory of global CO2 emissions in the long term is expected to be significantly influenced by governmental actions and economic incentives implemented in the aftermath of the crisis. These measures are anticipated to have a lasting impact for several decades (Arshad, 2020). Therefore, further research is needed to determine the long-term impact of the pandemic on CO_2 emissions and to develop sustainable strategies to reduce CO_2 emissions in the future.

Acknowledgment

The author is grateful for the satellite inversion data provided by the GOSAT Project and the daily CO_2 emissions data generated by the Global Carbon Project.

This project was supported by the scientific research program of the Hubei Provincial Department of Education under Grant No. D20191403 and by the College Student Innovation and Entrepreneurship Training Program of the Hubei University of Technology under Grant No. X202110500134.

Authors' contributions

WU Xulong: Data analysis and Manuscript writing.
Dan Xuefu: Manuscript revision.
Zhang Jinye: Supervision & project guidance.
Liu Ruibei: Technical supervision HU.
Ziyue: Data processing.
XU Chang: Data acquisition.

Disclaimer: The contents and views presented in this research article/paper are the views of the authors and do not necessarily reflect the views of the organizations they belongs to.

References

Arshad, A., 2020, "Temporary Reduction in Surface Water Pollution During the COVID-19 Forced Confinement-Case Study of Vembanad Lake and Coastal Regions".

Dacre, H. F., Western, L. M., Say, D., Doherty, S. O., Arnold, T., Rennick, C. and Hawkins, E., 2021, "Detectability of COVID-19 global emissions reductions in local CO_2 concentration measurements", *Environmental Research Letters,* https://doi.org/10.1088/1748-9326/ac1eda.

Fei Jiang, Wei He, WeiminJu, Hengmao Wang, Mousong Wu, Jun Wang, Shuzhuang Feng, Lingyu Zhang and Jing M. Chen, 2022, "The status of carbon neutrality of the world's top 5 CO_2 emitters as seen by carbon satellites", *Fundamental Research*. https://doi.org/10.1016/j.fmre.2022.02.001.

Houghton, J., 2009, "Global warming : the complete briefing", Cambridge university press.

Hwang, Y., Roh, J. W., Suh, D., Otto, M.-O., Schlueter, S., Choudhury, T., Huh, J.-S. and Um, J. -S., 2021, "No evidence for global decrease in CO_2 concentration during the first wave of COVID-19 pandemic", *Environmental Monitoring and Assessment*. https://doi.org/10.1007/s10661-021-09541-w.

Le Quéré, C., Jackson, R. B., Jones, M. W., Smith, A. J. P., Abernethy, S., Andrew, R. M., De-Gol, A. J., Willis, D. R., Shan, Y., Canadell, J. G., Friedlingstein, P., Creutzig, F. and Peters, G. P., 2020, "Temporary reduction in daily global CO_2 emissions during the COVID-19 forced confinement", *Nature Climate*

Change, **10**, 7, 647-653. https://doi.org/10.1038/s41558-020-0797-x.

Moersen, A., 2020, "Global emissions have dropped 17 percent during coronavirus pandemic". https://gritdaily.com/global-emissions-have-dropped-17-percent-during-coronavirus-pandemic/.

Parida, B. R., Bar, S., Singh, N., Oinam, B. and Kumar, M., 2020, "A short-term decline in anthropogenic emission of CO_2 in India due to covid-19 confinement", Progress in Physical Geography.

Quadrelli, R. and Peterson, S., 2007, "The energy-climate challenge: recent trends in CO_2 emissions from fuel combustion", *Energy Policy*, **35**, 11, 5938-5952.

Rugani, B. and Caro, D., 2020, "Impact of COVID-19 outbreak measures of lockdown on the Italian Carbon Footprint", *Science of The Total Environment*, **737**, 139806. https://doi.org/10.1016/j.scitotenv.2020.139806.

Shanshan, H., Liping, L. and Xiangjuan, G., 2013, "A general introduction to greenhouse gases observing satellite (GOSAT) and its products", *Remote Sensing Technology and Application*, **28**, 2, 269-275.

Sharma, L. K. and Verma, R. K., 2021, "Latitudinal fluctuation in global concentration of CO_2 and CH_4 from shortwave infrared spectral observation by GOSAT during COVID-19", *International Journal of Digital Earth*, **14**, 12, 1882-1896.

Simpkins, G., 2020, "COVID-19 carbon cuts", *Nature Reviews Earth & Environment*, **1**, 6, 279-279. https://doi.org/10.1038/s43017-020-0062-x.

The State Council Information Office of the People's Republic of China (SCIO), 2020, "Fighting Covid-19 : China in Action", available at http://english.www.gov.cn/ accessed on 20 Jan, 2022.

Tollefson, J., 2020, "How the coronavirus pandemic slashed carbon emissions - in five graphs", *Nature*, **582**, 158-159. https://doi.org/10.1038/d41586-020-01497-0.

World Health Organisation (WHO), 2022, "WHO Coronavirus (COVID-19) Dashboard", available at https://covid19.who.int/ accessed on 16 November, 2022.

Zhang, L. and Zhang, J., 2018, "Analysis of the Seasonal Variation of CO_2 Concentration in China Based on GOSAT Satellite Data", *Journal of the Indian Society of Remote Sensing*, **46**, 1667-1675.